

Re-examination of the $\text{N}_2\text{O} + \text{O}$ reaction

Peter Glarborg,^{*,†} Johanne S. Allingham,[†] Alexander B. Skov,[†] Hamid Hashemi,[†]
and Paul Marshall[‡]

[†]*DTU Chemical Engineering, Technical University of Denmark, 2800 Lyngby, Denmark*

[‡]*Department of Chemistry and Center for Advanced Scientific Computing and Modeling,
University of North Texas, 1155 Union Circle #305070, Denton, Texas 76203-5017*

E-mail: pgl@kt.dtu.dk

Abstract

The reaction of N_2O with O is a key step in consumption of nitrous oxide in thermal processes. It has two product channels, $\text{NO} + \text{NO}$ (R2) and $\text{N}_2 + \text{O}_2$ (R3). The rate constant for R2 has been measured both in the forward and the reverse direction at elevated temperature and is well established. However, the rate constant for the $\text{N}_2 + \text{O}_2$ channel (R3) has been difficult to quantify and has significant error limits. The direct reaction on the triplet surface has a barrier of around $40 \text{ kcal mole}^{-1}$ and it is too slow for the $\text{N}_2 + \text{O}_2$ channel to have any practical significance. Recently, Pham and Lin (2022) suggested an alternative low activation energy reaction path that involves inter-system crossing and reaction on the singlet surface. In the present work, we re-examined a wide range of experiments relevant for the $\text{N}_2\text{O} + \text{O}$ reaction through kinetic modeling, paying attention to the impact of artifacts such as impurities and surface reactions. Experimental results from shock tubes and batch reactors on the final NO yield in N_2O decomposition, covering temperatures of 973-2200 K and pressures of 0.013-11.5 atm, support $k_3 \sim 0$, consistent with the high activation energy for reaction on the triplet surface and a low probability of ISC.

Introduction

Challenges of using ammonia as a carbon-free fuel in engines and gas turbines are investigated extensively.¹⁻³ Concerns include poor ignition and combustion properties, as well as emissions of oxides of nitrogen. A particular concern is the formation of the strong greenhouse gas nitrous oxide (N_2O). Levels of just a few hundred ppm of N_2O in the exhaust are sufficient to offset the benefit of using a carbon-free fuel with respect to the greenhouse effect.

In diesel engines, the combustion of ammonia takes place at intermediate to high temperature and high pressure. Reaction of amine radicals with nitrogen oxides offers two routes to formation of N_2O ; a high temperature pathway involving the reaction $\text{NH} + \text{NO} \rightleftharpoons \text{N}_2\text{O} + \text{H}$ and a low temperature route via $\text{NH}_2 + \text{NO}_2 \rightleftharpoons \text{N}_2\text{O} + \text{H}_2\text{O}$.^{4,5} Nitrous oxide, once formed, may be consumed by thermal dissociation,



or by reaction with the O/H radical pool, in particular atomic oxygen and atomic hydrogen.⁴ The $\text{N}_2\text{O} + \text{O}$ reaction has two product channels,



The rate constant for forming $\text{NO} + \text{NO}$ (R2) has been measured both in the forward and reverse directions at elevated temperature and is believed to be well established.^{6,7} However, the rate constant for the $\text{N}_2 + \text{O}_2$ channel has significant error limits.⁷ In early evaluations by Baulch et al.,⁸ Hanson and Salimian,⁹ and Tsang and Herron,¹⁰ it was concluded that k_2 and k_3 were similar over a wide temperature range, both with an activation energy of around 28 kcal mol^{-1} . In subsequent work, this finding has been questioned. Davidson et

al.¹¹ measured NO and O₂ in shock tube experiments on N₂O decomposition, reporting a significantly lower activation energy of 15.9 kcal mol⁻¹ for R3. This result was supported by the direct measurements of N₂O + O by Fontijn et al.¹² and by the re-examination of available experimental results by Meagher and Anderson.⁶ A small activation energy for R3 would cause formation of N₂ + O₂ to dominate at lower temperatures, while NO formation would dominate at temperatures above 1840 K. Further support for a low activation energy for R3 was recently provided by Pham et al.¹³ from static reactor experiments.

From theoretical work, it is known that the direct reaction on the triplet surface has a high barrier that would make it too slow for the N₂ + O₂ channel to have any practical significance. Gonzalez et al.¹⁴ calculated a barrier of 38.5 kcal mol⁻¹ on the triplet surface, while Pham and Lin¹⁵ reported a value of 41.3 kcal mol⁻¹. However, Pham and Lin proposed that reaction R3 may proceed on the singlet surface following inter-system crossing (ISC); this would involve an activation energy of only 12.9 kcal mol⁻¹.

The importance of the N₂ + O₂ channel is still in question, however. Experimental results from batch reactors,¹⁶ premixed flames,¹⁷ and shock tubes,¹⁸ appear to conflict with a low barrier pathway, and Glarborg et al.⁴ argued that R3 should have an activation energy of at least 28 kcal mol⁻¹, in agreement with the early evaluations.⁸⁻¹⁰ Even though the N₂O + O reaction in general is less important for consuming N₂O in combustion than thermal dissociation and reaction with H, the issue about the rate constant for R3 needs to be resolved. If this step has a low barrier pathway, it will promote N₂O consumption under the lean, low-temperature conditions late in the engine cycle. Furthermore, the N₂O + O reaction is important for interpretation of experimental results on N₂O dissociation and for kinetic studies that rely on N₂O as the O atom source. The conflicting experimental results on the rate constants for the N₂O + O reaction cannot be reconciled in terms of a better understanding of the details of the N₂O decomposition chemistry, but must partly be attributed to experimental artifacts. While a low activation energy pathway would be possible due to inter-system crossing,¹⁵ rate constants for reactions involving ISC are difficult to quantify.

In the present work, we re-examine experiments relevant for the $\text{N}_2\text{O} + \text{O}$ reaction through kinetic modeling to evaluate the importance of the $\text{N}_2 + \text{O}_2$ product channel.

Kinetic model

We interpret selected experiments from literature, relevant for $\text{N}_2\text{O} + \text{O}$, in terms of a detailed chemical kinetic model. The rate coefficients and thermodynamic data were drawn mainly from the review of nitrogen chemistry by Glarborg et al.⁴ However, the N_2O subset was updated as discussed below. The mechanism includes reactions in the hydrogen oxidation system, as H_2O is present in some experiments as an impurity. Table 1 lists selected reactions from the N_2O reaction subset, including estimated uncertainty factors. The full mechanism is available as Supplementary Material.

The dissociation of N_2O (R1) has been studied experimentally over a wide range of conditions. We have adopted the recommendation of Baulch et al.⁷ for the low and high pressure limits. Their low-pressure limit agrees within 20% with the more recent determinations by Savoy et al.²² and Mulvihill et al.²³ Since some of the investigated experiments in the present work were conducted with high concentrations of N_2O , the collision efficiency of N_2O in R1 becomes important. Based on the batch reactor results from Johnston,²⁴ Lindars and Hinshelwood,²⁵ and Kaufman et al.,¹⁶ and the evaluation of Baulch et al.,⁸ we estimate a third-body efficiency of N_2O compared to Ar of 6 (see Fig. 1).

Among the two product channels for the $\text{N}_2\text{O} + \text{O}$ reaction,



the rate constant for forming $\text{NO} + \text{NO}$ (R2) is well established.^{6,7} Figure 2 shows an

Table 1: Key reactions in the N₂O mechanism. Parameters for use in the modified Arrhenius expression $k = AT^\beta \exp(-E/[RT])$. Units are mol, cm, s, cal. The resulting rate constant for R4 is the sum of the two listed rate constants. UF is the estimated uncertainty factor, mainly based on the evaluations of Baulch and coworkers^{7,8} and Meagher and Anderson.⁶

	A	β	E	UF	Source
1. N ₂ O(+M) \rightleftharpoons O + N ₂ (+M)	9.9E10	0.000	57901	3	⁷
Low pressure limit:	6.0E14	0.000	57444	1.5-3 ^a	
Collision efficiencies: N ₂ =1.7, O ₂ =1.4, H ₂ O=12, N ₂ O=6					
2. N ₂ O + O \rightleftharpoons NO + NO	2.0E10	1.000	24800	1.5	¹⁴
3. N ₂ O + O \rightleftharpoons N ₂ + O ₂	2.6E12	0.500	41100	–	¹⁴
4. N ₂ O + H \rightleftharpoons N ₂ + OH	6.7E10	0.000	5385	2	¹⁹
Duplicate	4.4E14	0.000	18900		
5. N ₂ O + OH \rightleftharpoons N ₂ + HO ₂	1.3E-2	4.720	36560	10	²⁰
6. N ₂ O + OH \rightleftharpoons HNO + NO	1.2E-4	4.330	25080	10	²⁰
7. NO + O(+M) \rightleftharpoons NO ₂ (+M)	1.3E15	-0.750	0	3	⁴ , pw
Low pressure limit (N ₂):	4.72E24	-2.870	1550	2	
Low pressure limit (Ar):	7.56E19	-1.410	0	2	
Collision efficiencies: N ₂ =1, N ₂ O=3 ^b					
8. NO ₂ + O \rightleftharpoons NO + O ₂	1.1E14	-0.520	0	2-4 ^c	²¹

a: The uncertainty factors for Ar and N₂ are 1.5-2.0, while for N₂O as collision partner UF is increased to a value of 3.

b: For N₂O as collision partner, UF = 3.

c: The uncertainty factor is 2 below 1000 K, increasing to 4 at high temperature.

Arrhenius plot for R2. The rate constant has been measured in both the forward and the reverse direction at elevated temperature, mostly in shock tube experiments. The ratio of forward and reverse rate constants matches the thermodynamic equilibrium constant. The main uncertainties in deriving k_2 involve the impact of the N₂ + O₂ channel (R3) and the presence of impurities, in particular H₂O. Most of the data selected for the figure were obtained from measurements of the reverse step,



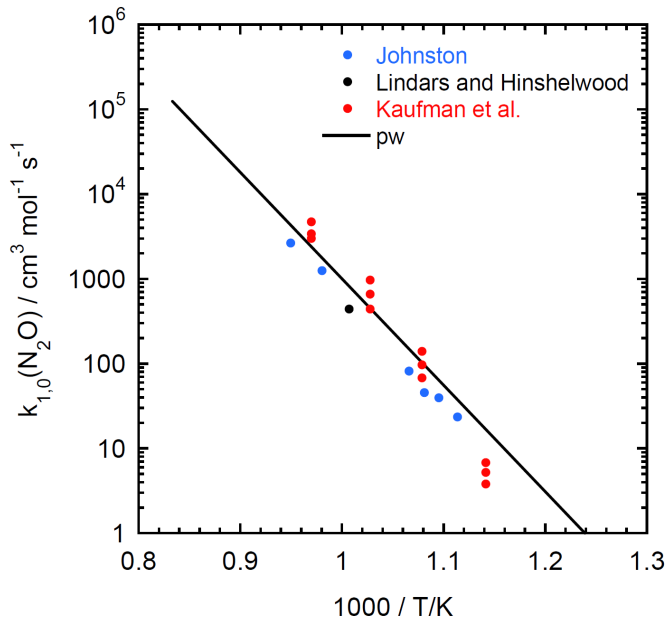


Figure 1: Arrhenius plot for the reaction $\text{N}_2\text{O} + \text{N}_2\text{O} \rightleftharpoons \text{N}_2 + \text{O} + \text{N}_2\text{O}$ (R1). The closed symbols denote measurements from batch reactor experiments, while the solid line denotes the value preferred in the present work, corresponding to a collision efficiency of N_2O compared to Ar of 6. The experimental data were drawn from Johnston,²⁴ Lindars and Hinshelwood,²⁵ and Kaufman et al.,¹⁶ as derived by Baulch et al.⁸

Results for R2b are not affected by the uncertainty in k_3 and, additionally, are less sensitive to impurities. Rate constants for R2b have been obtained from shock tubes,^{26,27} flow reactors,²⁸ and batch reactors,^{29,30} and they cover a wide temperature range. The data are consistent with the shock tube measurements for k_2 from Monat et al.³¹ and Davidson et al.,¹¹ and for $k_{\text{tot}} = k_2 + k_3$ of Dean and Stephens,³² assuming k_3 to be negligible. Furthermore, the measurements agree well with the recommendation of Meagher and Anderson⁶ and the theoretical values from Gonzalez et al.¹⁴ and Pham and Lin¹⁵ (the latter not shown). Meagher and Anderson based their recommendation of k_2 on, among others, measurements of Monat et al.,³¹ Zaslanko and coworkers,^{33,34} and Davidson et al.¹¹ in the forward direction, and in the reverse direction ($\text{NO} + \text{NO}$) Kaufman and Kelso,³⁰ McCullough et al.,²⁸ Koshi and Asaba,²⁶ and Thielen and Roth.²⁷

Also shown in Fig. 2 are the upper limit values for k_{tot} reported by Ross et al.³⁵ They measured O-atom concentrations by ARAS in shock tube N_2O decomposition experiments.

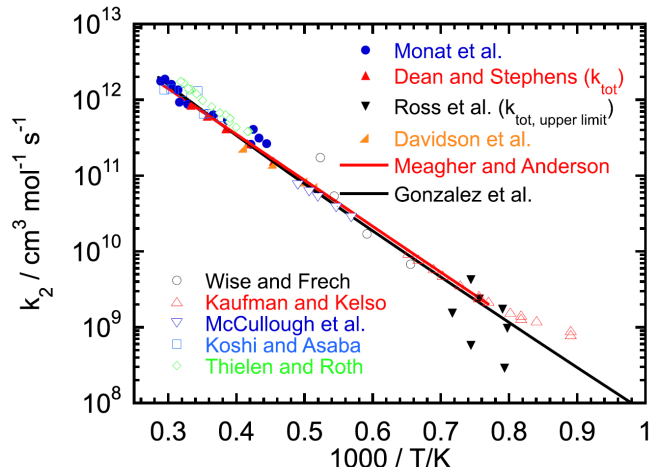


Figure 2: Arrhenius plot for the reaction $\text{N}_2\text{O} + \text{O} \rightleftharpoons \text{NO} + \text{NO}$ (R2). The closed symbols denote measurements of the forward reaction while the open symbols denote data obtained from measurements of the reverse step, converted using the thermodynamic properties. Data for k_2 : Monat et al.,³¹ Davidson et al.,¹¹ Dean and Stephens³² ($k_{\text{tot}} = k_2 + k_3$), and Ross et al.³⁵ (k_{tot} , upper limit). Data derived from measurements of k_{2b} : Wise and Frech,²⁹ Kaufman and Kelso,³⁰ McCullough et al.,²⁸ Koshi and Asaba,²⁶ and Thielen and Roth.²⁷ The solid lines show the theoretical value from Gonzalez et al.¹⁴ and the recommendation of Meagher and Anderson,⁶ respectively. The upper limit for k_{tot} by Ross et al.³⁵ shown in the figure is their original value multiplied by the reported uncertainty of a factor of three.

The lack of curvature in the O-profile was interpreted in terms of a low overall rate constant for $\text{N}_2\text{O} + \text{O}$. They attributed an uncertainty of a factor of three to their reported upper limit; to obtain a conservative upper limit, we have multiplied their values by 3 in Fig. 2.

Figure 3 shows an Arrhenius plot for R3. We have omitted most of the reported shock tube determinations due to concerns about impurities, as discussed below. The data from Davidson et al.¹¹ are shown, along with the batch reactor results of Pham et al.,¹³ the data of Fontijn et al.¹² for k_{tot} , and the upper limit value for k_{tot} from Ross et al.³⁵ The figure also includes the recommendations from Hanson and Salimian⁹ (close to those of Baulch et al.⁸ and Tsang and Herron¹⁰) and Meagher and Anderson,⁶ as well as the theoretical values from Gonzalez et al.¹⁴ and Pham and Lin.¹⁵ The Meagher and Anderson recommendation for k_3 was adopted in the more recent evaluation by Baulch et al.,⁷ but assigned significant error margins.

Fontijn et al.¹² measured directly the overall rate constant for $\text{N}_2\text{O} + \text{O}$ (k_{tot}) by mon-

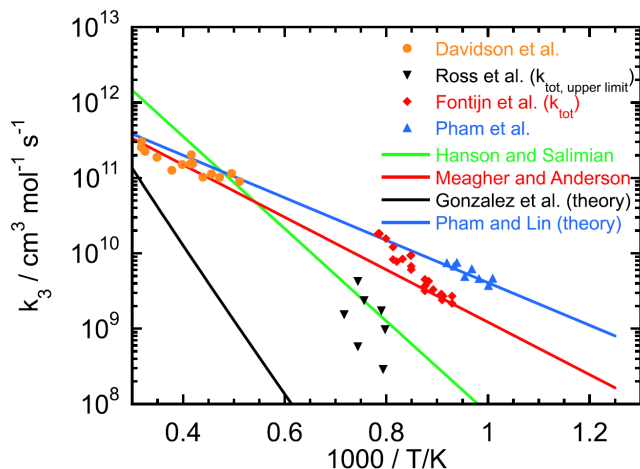


Figure 3: Arrhenius plot for the reaction $\text{N}_2\text{O} + \text{O} \rightleftharpoons \text{N}_2 + \text{O}_2$ (R3). The symbols denote selected measurements of the reaction, while solid lines denote evaluations or theoretical values. Measurements: Davidson et al.,¹¹ Ross et al.³⁵ ($k_{\text{tot}} = k_2 + k_3$, upper limit), Fontijn et al.¹² (k_{tot}), and Pham et al.¹³ Evaluations: Hanson and Salimian⁹ and Meagher and Anderson.⁶ Theoretical values: Gonzalez et al.¹⁴ and Pham and Lin.¹⁵ The upper limit for k_{tot} by Ross et al.³⁵ shown in the figure is their original value multiplied by the reported uncertainty of a factor of three.

itoring $[\text{O}]$. Their derived rate constant, shown in Fig. 3, is too high to be compatible with values for k_2 (Fig. 2). As a result, discussed in detail in the accompanying paper by Meagher and Anderson,⁶ Fontijn et al. attributed their measurement to reaction R3.

The reported values of k_3 shown in Fig. 3 vary over several orders of magnitude. The data from Pham et al. and Fontijn et al. are clearly incompatible with the upper limit values for k_{tot} reported by Ross et al.³⁵ The experiments of Fontijn et al. were difficult to conduct due to a high sensitivity to impurities. They carefully analyzed the potential water effect, stating that the presence of just 5 ppm H_2O would allow their measurements to be interpreted in terms of the Hanson and Salimian rate constants for $\text{N}_2\text{O} + \text{O}$, involving a much lower value of k_3 . Also the presence of NO , formed from N_2O dissociation prior to the flash photolysis, was a concern due to the O-removal by the sequence $\text{NO} + \text{O} (+\text{M}) \rightarrow \text{NO}_2 + \text{M}$ (R7), $\text{NO}_2 + \text{O} \rightarrow \text{NO} + \text{O}_2$ (R8). However, Fontijn et al. concluded that their results were reliable, at least at the lower temperatures, with H_2O well below 5 ppm. A potential, unrecognized difficulty with those experiments is that the laser photolytic generation of $\text{O}(^3\text{P})$ from SO_2

at 193 nm will also generate $O(^1D)$ from N_2O . In competition with quenching by the Ar bath gas, $O(^1D)$ will react quickly with N_2O to yield further NO.

In the present work, we tentatively adopt the values of both k_2 and k_3 from the theoretical work of Gonzalez et al.¹⁴ The sum of these values complies roughly with the upper limit for k_{tot} by Ross et al.³⁵ shown in Fig. 3 (i.e., multiplied by a factor of 3). However, the rate constant for R3 is significantly lower than values currently used in modeling.^{4,6,9} In the following, the implications of experimental results reported in the literature for the value of k_3 are investigated.

In Table 1, also the reactions $NO + O (+M) \rightarrow NO_2 + M$ (R7) and $NO_2 + O \rightarrow NO + O_2$ (R8) are listed. They are important for consuming atomic oxygen, once NO has been formed in reaction R2. Note that for NO_2 dissociation (R7), we have assumed a collision efficiency of N_2O compared to N_2 of 3 (roughly 6 compared to Ar), consistent with the value discussed above for R1. For $NO_2 + O$ (R8), the measurements of Bemand et al.²¹ (298-1060 K) and Bedjanian and Kalyan³⁶ (220-950 K) show a slight negative temperature dependence. A recent theoretical study by Li et al.³⁷ indicates a sharp increase in the rate constant above 1000 K, but this is not confirmed by direct measurements.

Results and Discussion

Experimental data relevant for quantification of k_3 have been reported from shock tubes, batch reactors, flow reactors, and laminar, premixed flames. Through a screening process, the reliability of the results were evaluated and experiments were selected for re-examination. The issues with the different types of experiments are discussed in detail below. Some of the early shock tube work may have been affected by water vapor impurities, and, in line with Meagher and Anderson,⁶ we chose to discard most of these results. Also, data obtained in the presence of combustibles like H_2 and CO were disregarded due to the increased importance of secondary reactions such as $N_2O + H$. These include the laminar premixed flame results

of Fenimore and Jones³⁸ ($\text{H}_2/\text{N}_2\text{O}/\text{Ar}$ flames) and Dindi et al.¹⁷ ($\text{CO}/\text{N}_2\text{O}/\text{Ar}$ flames).

Shock tube experiments

The decomposition of N_2O has been studied extensively in shock tubes.^{11,22,23,31-35,39-51} A number of these studies have involved determination of rate constant and/or branching fraction for the $\text{N}_2\text{O} + \text{O}$ reaction.^{11,31-35,39,43-49} The results should be interpreted cautiously because they may have been affected by experimental artifacts. Concerns include boundary layer effects, thermal effects, and impurities. Since the $\text{N}_2\text{O} + \text{O}$ reaction is comparatively slow compared to $\text{N}_2\text{O} + \text{H}$, the experiments are particularly sensitive to trace amounts of hydrogen or water vapor.

In current state-of-the-art shock tube measurements, water vapor impurities have largely been eliminated by using very low base pressures (typically $<10^{-8}$ atm) together with other measures to minimize contaminants from ambient air and to suppress potential wall adsorption effects. However, early shock tube experiments possibly had issues with H_2O contamination. Zuev and Starikovskii⁵² cite a mass spectrometric study by Kondrashov et al. (1984, in Russian) who determined that the water vapor concentration in the prepared mixture could increase substantially as a result of H_2O desorption from the reactor walls. After pumping out the test section of the shock tube to $2 \cdot 10^{-5}$ atm and rinsing with He, the initially dry mixture contained 100-500 ppm H_2O after 10 min in the shock tube.⁵² It has been known since the late 1970's that minimizing the time between the introduction of the reactant mixture in the shock tube and triggering the shock could limit the H_2O contamination to below 10 ppm or better.^{22,32,48} However, a significant part of the shock tube work on $\text{N}_2\text{O} + \text{O}$ dates back before this time.

The issue with water vapor impurities has implications also for the study of other slow reactions, for example those of CO with O_2 , SO_2 , and N_2O . Several shock tube studies have been reported on N_2O decomposition in the presence of CO.^{32,34,48,53-57} The results of Milks and Matula⁵⁴ and others^{53,55,56} were interpreted in terms of a low activation energy for CO

+ N₂O of around 20 kcal mol⁻¹. This value conflicts with more recent experimental^{57,58} and theoretical⁵⁹ work, all of which support activation energies of around 40 kcal mol⁻¹. Dean and coworkers,^{32,48} who carefully controlled water vapor impurities, did not observe any acceleration of the N₂O decomposition rate in the presence of CO. Presumably, the observed low activation energy for CO + N₂O can be attributed to trace amounts of water vapor enhancing the consumption rate of CO. Similar issues have been identified for shock tube studies of the CO + SO₂ reaction.⁶⁰

Since O₂ is difficult to quantify in small concentrations, most studies of R3 are indirect, relying on measurements of NO. In Fig. 4, the impact of trace amounts of H₂O on the NO yield in decomposition of 3% N₂O in Ar in a shock tube is displayed. Modeling predictions are compared to experimental data from Zaslanko et al.³³ and Lipkea et al.⁴⁶ It can be assumed that the data from Lipkea et al. had issues with impurities, being from the same batch of experiments as those of Milks and Matula on CO + N₂O,⁵⁴ and they were discarded by Meagher and Anderson.⁶ The agreement between the experimental results from Zaslanko et al. and Lipkea et al. leads us to believe that also the results from Zaslanko et al. were affected by impurities.

Based on their measurements, Zaslanko et al. and Lipkea et al. proposed values of $k_2/(k_2+k_3)$ in the range 0.3-0.5. In the present model, with the preferred values of k_2 and k_3 from Gonzalez et al.,¹⁴ this ratio is close to 1.0. Consequently, the NO yield is strongly overpredicted under dry conditions. However, the calculated NO yield is sensitive to trace amounts of H₂O. Levels of 200-300 ppm H₂O are sufficient to explain the measurements in terms of the very low value of k_3 calculated by Gonzalez et al. (triplet surface). Possibly, the early shock tube results that were the basis for the evaluations by Baulch et al.,⁸ Hanson and Salimian,⁹ and Tsang and Herron¹⁰ on k_3 had significant error margins.

In more recent shock tube investigations, precautions were taken to minimize the issues with impurities. Figure 5 compares modeling predictions with the measured NO reported by Zuev and Starikovskii,⁵² who reported results over a wide range of temperature (1800-2500

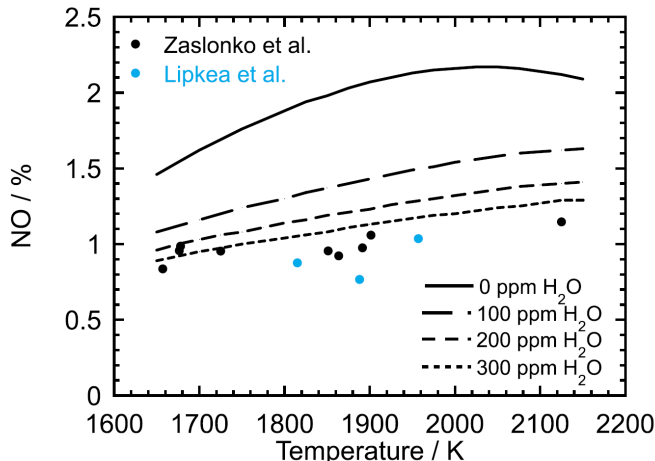


Figure 4: Comparison of the experimental data of Zaslanko et al.³³ and Lipkea et al.⁴⁶ with modeling predictions for formation of NO in decomposition of 3% N₂O in Ar in a shock tube as a function of temperature at a pressure of about 2 atm. Symbols denote experimental data, while lines denote modeling predictions for different trace amounts of water vapor.

K) and pressure (2.5-22.5 atm). At lower temperatures, i.e., 1800-1900 K, they observed heating of the reacting gas corresponding to the adiabatic temperature increase of about 50 K. However, at higher temperatures, boundary layer effects caused a significant cooling of the reactant gas; 50 K at 2200 K and 150 K at 3300 K at 10 atm. For this reason, data obtained above 2200 K have been omitted in Fig. 5. The results show that NO increases slightly with temperature, but decreases with pressure. The NO yield results from competition for O between N₂O + O (R2, R3) and the sequence NO + O (+M) → NO₂ + M (R7) and NO₂ + O → NO + O₂ (R8). A higher temperature promotes N₂O + O forming NO (R2), while increased pressure favors the NO/NO₂ interconversion.

Modeling predictions are shown for values of k_3 from both Gonzalez et al. and Meagher and Anderson. Use of the low rate constant for R3 from Gonzalez et al. results in good agreement with experiment over the range of temperature and pressure investigated, while the value from Meagher and Anderson causes a significant underprediction of NO.

Figure 6 compares modeling predictions with experimental data from Ross et al.³⁵ They measured O atom profiles in decomposition of 2000 ppm N₂O in Ar at intermediate temperatures, here 1395 K. The results are of particular interest because they are obtained at

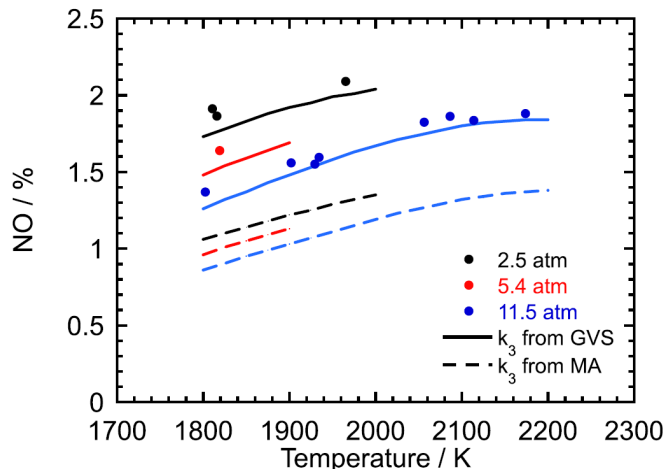


Figure 5: Comparison of the experimental data of Zuev and Starikovskii⁵² with modeling predictions for formation of NO in decomposition of 3% N₂O in Ar in a shock tube as a function of temperature and pressure. Symbols denote experimental data, while lines denote modeling predictions with k_3 from Gonzalez et al.¹⁴ and Meagher and Anderson,⁶ respectively.

temperatures where R3 dominates, according to Meagher and Anderson.

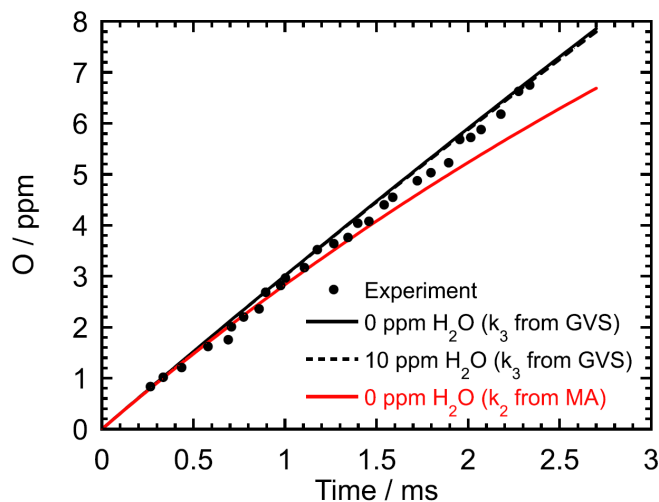


Figure 6: Comparison of the measured and predicted O atom profile in decomposition of 2000 ppm N₂O in Ar in a shock tube at 1395 K and 0.61 atm. The experimental data, shown as symbols, are from Ross et al.³⁵ Solid and dashed lines denote modeling predictions with k_3 from Gonzalez et al.¹⁴ and from Meagher and Anderson,⁶ respectively, at varying trace levels of H₂O. The low-pressure limit $k_{1,0}$ for N₂O + Ar was lowered by 50% in the modeling to match the early O formation rate in the experiment.

The measured O-atom profile is linear in time. This indicates that [O] is controlled by

formation via $\text{N}_2\text{O} (+\text{M})$ (R1), while consumption by secondary reactions such as $\text{N}_2\text{O} + \text{O}$ (R2, R3) has little impact. Ross et al. interpreted their results in terms of upper limits for $k_{\text{tot}} = k_2 + k_3$. Use of the rate constants for R2 and R3 from Gonzalez et al., which comply roughly with these upper limits, results in good agreement with experiment. Contrary to this, the value from Meagher and Anderson causes a significant curvature in the predicted O-profile. It should be noted that for these conditions low levels of H_2O impurities have no impact on predictions.

The shock tube work of Davidson et al.¹¹ was considered by Meagher and Anderson to provide support for a low activation energy channel for R3. Davidson et al. measured NO and O_2 in shock tube experiments on N_2O decomposition, deriving values of k_2 (1680-2430 K) and k_3 (1940-3340 K). Their results for k_2 are consistent with other work (Fig. 2), even though the proposed activation energy of 23 kcal mol⁻¹ conflicts with the generally accepted value of 28 kcal mol⁻¹.^{6,7}

Figure 7 compares the NO mole fraction profile measured by Davidson et al. in decomposition of 5350 ppm N_2O in Ar at 1868 K and 1.09 atm with modeling predictions. The measurement of NO was complicated by an interference with N_2O (which was not quantified). However, it is noteworthy that the present rate constants for $\text{N}_2\text{O} + \text{O}$ from Gonzalez et al. provide a good agreement with experiment, while use of k_3 from Meagher and Anderson results in underprediction of NO. The calculations indicate that trace amounts of water vapor in the range 5-10 ppm would be consistent with the experimental observations.

Due to a low signal-to-noise ratio for the O_2 signal, Davidson et al. had to increase the starting concentration of N_2O to quantify $[\text{O}_2]$. Furthermore, they could not obtain data below 2000 K, where R3 was supposed to dominate. Figure 8 compares measured and predicted O_2 mole fractions in decomposition of 2.34% N_2O at 2268 K. Unlike the comparisons in the previous figures, use of k_3 from Meagher and Anderson here provides the best prediction, while the rate constant for R3 from Gonzalez et al. leads to underestimation of O_2 . The introduction of trace H_2O improves the agreement, but the expected impurity

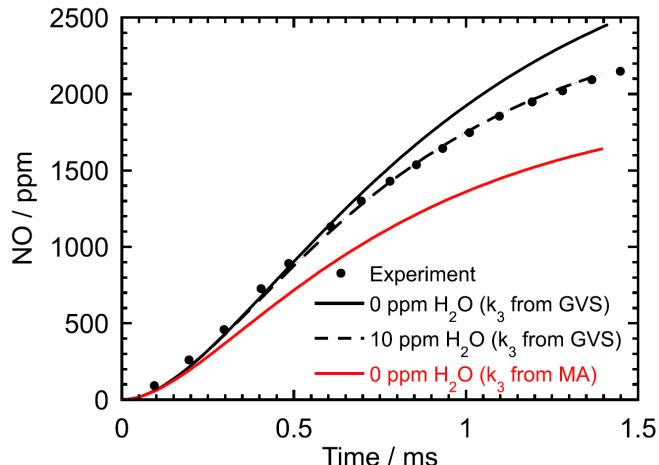


Figure 7: Comparison of the measured and predicted NO mole fractions in decomposition of 5350 ppm N₂O in Ar in a shock tube at 1868 K and 1.09 atm. The experimental data, shown as symbols, are from Davidson et al.¹¹ The NO detection had an increased uncertainty due to cross-interference with N₂O. Lines denote modeling predictions with k_3 from Gonzalez et al.¹⁴ and from Meagher and Anderson⁶ at varying trace levels of H₂O.

level of 5-10 ppm is not sufficient to reconcile the predictions with experiment. Based on the present mechanism and accounting for 10 ppm H₂O as impurity, that would require $k_3 \sim 4 \cdot 10^{10} \text{ cm}^3 \text{ mol}^{-1} \text{ s}^{-1}$. At 2268 K, this value is 3-5 times below the recommendations of Davidson et al., Meagher and Anderson,⁶ and Pham and coworkers.^{13,15}

Batch reactor experiments

Data for the NO yield in N₂O decomposition have been reported from a number of batch reactor studies.^{16,25,61,62} The most reliable data were reported by Kaufman et al.,¹⁶ who measured simultaneously N₂O and NO. They derived a value for the ratio k_2/k_3 based on the initial rates for $d[\text{N}_2\text{O}]/dt$ and $d[\text{NO}]/dt$, finding that the NO producing channel (R2) for $\text{N}_2\text{O} + \text{O}$ constituted 50-65% under these conditions (875-1030 K, varying pressure). Meagher and Anderson discarded these results due to the difficulty in extracting reliably the initial rates, combined with concerns about the early thermal equilibration. We agree with this assessment. However, the experimental results after the initial stage, in particular the final NO yield upon depletion of N₂O, may provide important information. While the

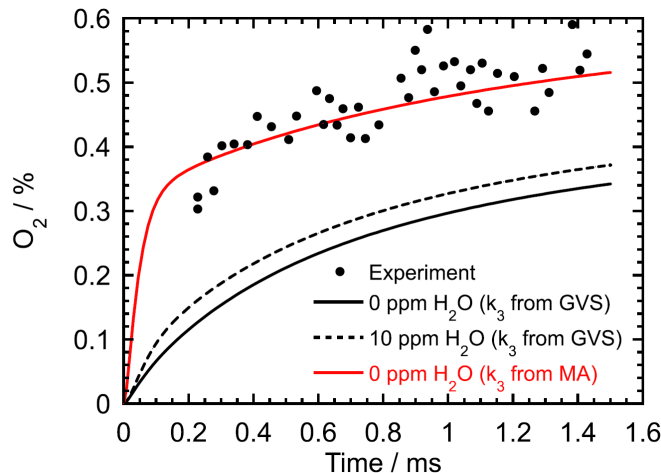


Figure 8: Comparison of the measured and predicted O_2 mole fraction in decomposition of 2.34% ppm N_2O in Ar in a shock tube at 2268 K and 1.67 atm. The experimental data, shown as symbols, are from Davidson et al.¹¹. Solid and dashed lines denote modeling predictions with k_3 from Gonzalez et al.¹⁴ and from Meagher and Anderson,⁶ respectively, at varying trace levels of H_2O .

sensitivity towards impurities would be small since the batch reactor experiments were conducted with high concentrations of nitrous oxide, the impact of surface reactions needs to be addressed.

Reactions on the reactor surface may act to decompose N_2O and to remove radicals, in this case atomic oxygen. There is evidence that decomposition of N_2O in quartz or pyrex batch reactors may have a heterogeneous component, particularly at lower temperature and pressure.^{24,61,63,64} Notably, observations of N_2O decomposition over quartz sand⁶⁵ indicate that any heterogeneous decomposition forms N_2 rather than NO . The experiments considered in the present analysis, by Lindars and Hinshelwood²⁵ and Kaufman et al.,¹⁶ were conducted in spherical reactors with a low surface/volume ratio. Based on varying the S/V ratio and the condition of the surface, both groups concluded that heterogeneous loss of N_2O had little impact in empty, seasoned reactors. This is supported by the observation that the activation energy derived for N_2O dissociation (R1) from the batch reactor experiments is consistent with a homogeneous reaction (see Fig. 1).

The other concern is loss of atomic oxygen on the reactor surface. Kaufman et al.¹⁶

reported that an increase in the surface/volume ratio by filling the reactor resulted in a decrease, not an increase, in formation of NO; an observation consistent with loss of O-atoms at the reactor surface at high S/V ratios. An upper limit for the O-consumption at the wall can be estimated by assuming it to be diffusion controlled. Such a reaction is included in our modeling, approximated as a simple first-order reaction.⁶⁶ We find that in empty reactors, the heterogeneous loss of O was small at pressures above 100 torr, while in the range 10-100 torr it had to be accounted for.

Based on our analysis, we conclude that the batch reactor results should be interpreted with care due to concerns about surface effects, but not discarded. We further note that to the extent any heterogeneous reaction occurs (loss of N₂O or O), it will suppress the NO yield rather than promote it. Figure 9 compares experimental data from Kaufman et al.¹⁶ on decomposition of pure nitrous oxide at 973 K and 50 torr. In this experiment, both N₂O and NO were monitored as a function of time.

The modeling was conducted with values of k_3 from Gonzalez et al.,¹⁴ Meagher and Anderson,⁶ and Pham and Lin.¹⁵ The surface loss of O was estimated as a function of reactor diameter, temperature, and pressure. Predictions with the preferred value of the rate constant for N₂O(+M) (R1), i.e., with a collision efficiency of N₂O compared to Ar of 6, together with k_3 from Gonzalez et al., results in a very good prediction of both N₂O and NO. Use of the rate constants for R3 from Meagher and Anderson and Pham and Lin both causes a severe underprediction of NO. Since experimental artifacts would tend to reduce the observed NO yield, these data strongly support a low value of k_3 .

The results show that the NO formation rate is high in the beginning, but then decreases as the NO concentration builds up. As was the case for the shock tube conditions discussed above, this is caused by the competition for atomic oxygen between N₂O + O (R2, R3) and the NO/NO₂ interconversion through NO + O (+M) → NO₂ + M (R7) and NO₂ + O → NO + O₂ (R8). In the batch reactor experiments with pure nitrous oxide, reaction R7 is promoted by the larger collision efficiency of N₂O compared to N₂.

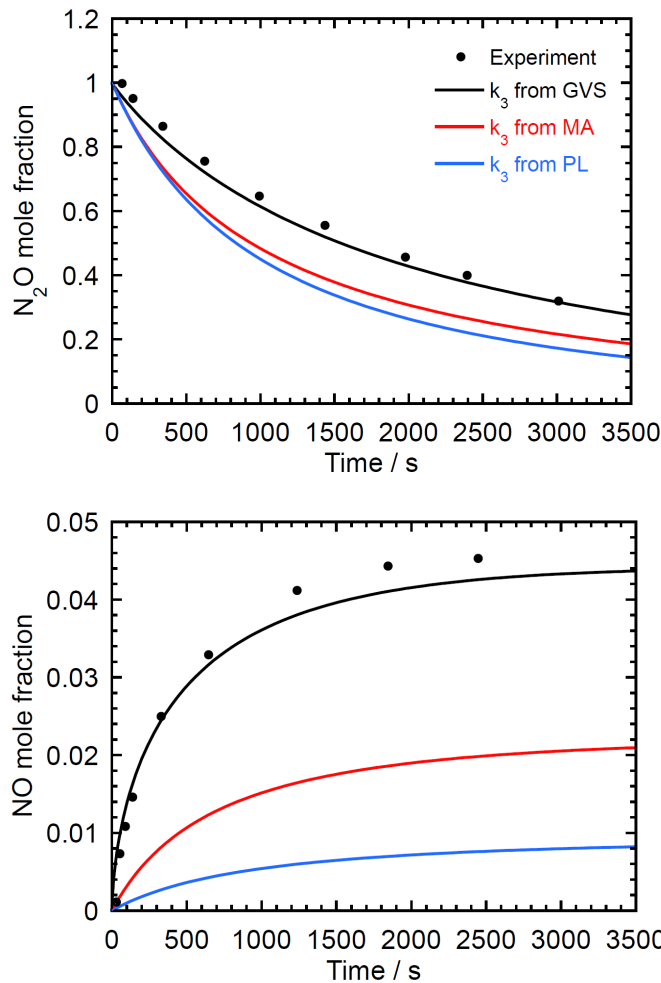


Figure 9: Comparison of the experimental data of Kaufman et al.¹⁶ with modeling predictions for N₂O and NO mole fractions in decomposition of pure N₂O in a batch reactor at 973 K and a pressure of 50 torr. Symbols denote experimental data, while lines denote modeling predictions with k_3 from Gonzalez et al.,¹⁴ Meagher and Anderson,⁶ and Pham and Lin,¹⁵ respectively. The modeling was conducted assuming constant temperature and volume.

Figure 10 compares the batch reactor data from Lindars and Hinshelwood²⁵ and Kaufman et al.,¹⁶ respectively, with modeling predictions for the final NO yield in decomposition of N₂O. The Lindars and Hinshelwood data were obtained at 993 K and 150-500 torr, compared to 1031 K and 10-200 torr for the results from Kaufman et al.¹⁶ The observed NO level is seen to decrease strongly with pressure. Even though less O is lost at the surface, the main effect of raising the pressure is to promote the NO + O (+M) reaction (R7), resulting in a decreasing yield of NO. Over the whole range of pressure (10-500 torr), modeling predictions

are in excellent agreement with experiment provided the k_3 value from Gonzalez et al. is used. Again, use of the rate constants from Meagher and Anderson and Pham and Lin, respectively, results in a significant underprediction of the NO yield.

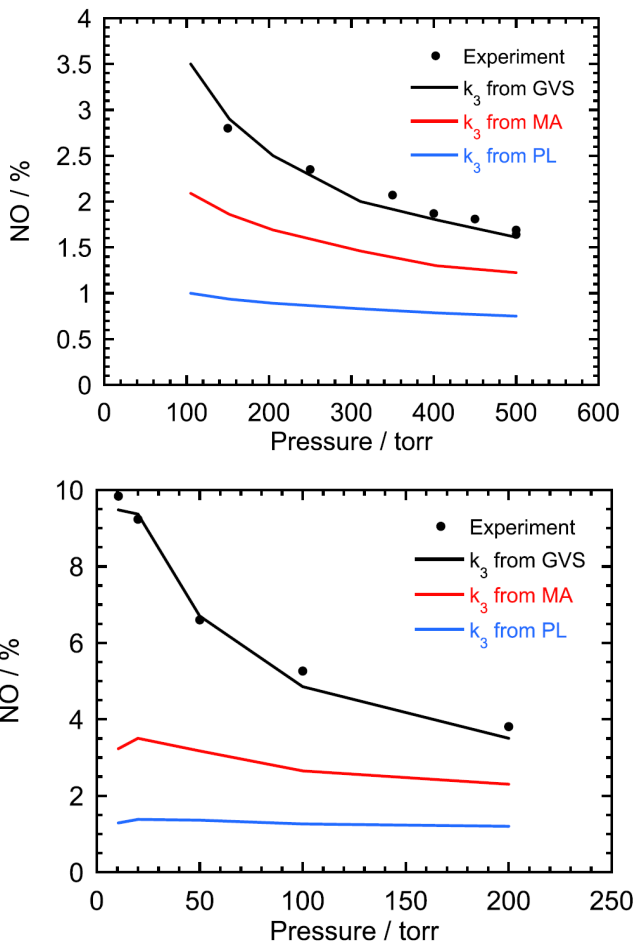


Figure 10: Comparison of the experimental data of Lindars and Hinshelwood²⁵ (upper figure, 993 K) and Kaufman et al.¹⁶ (lower figure, 1031 K) with modeling predictions for the final NO yield in full decomposition of pure N_2O in a batch reactor at varying pressure. Symbols denote experimental data, while lines denote modeling predictions with k_3 from Gonzalez et al.,¹⁴ Meagher and Anderson,⁶ and Pham and Lin,¹⁵ respectively. The modeling was conducted assuming constant temperature and volume.

Unlike the other batch reactor studies, the recent experiments of Pham et al.¹³ were interpreted in terms of a large rate constant for R3. Pham et al. conducted their measurements at higher pressure (800 torr) and dilute conditions. Data for NO were obtained in the temperature range 988-1083 K and initial N_2O levels of 7-10%. Our analysis supports

the claim by Pham et al. that their experimental results were not affected by impurities or loss of oxygen atoms at the reactor wall. Figure 11 compares their data for NO at 1083 K with modeling predictions. Surprisingly, the predictions with k_3 from Gonzalez et al. provide the best agreement with experiment, while the values from Meagher and Anderson and Pham and Lin lead to underestimation of the NO yield. Also the original 5-step mechanism from Pham et al. was tested, providing a significantly better prediction than the present mechanism with k_3 drawn from the theoretical study of Pham and Lin.

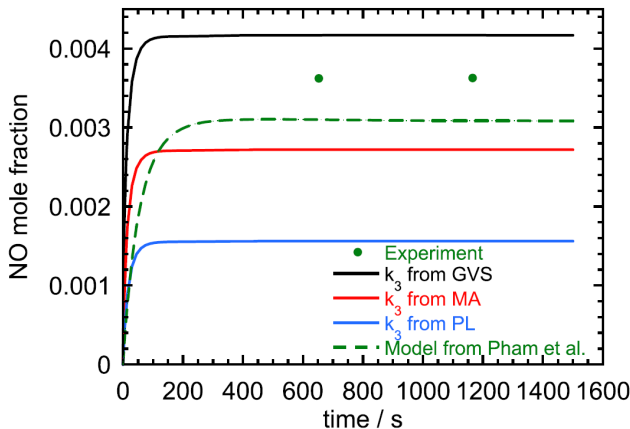


Figure 11: Comparison of the experimental data of Pham et al.¹³ with modeling predictions for the NO yield in decomposition of 7.1% N_2O in Ar in a batch reactor at 1083 K and a pressure of 800 torr. Symbols denote experimental data, while lines denote modeling predictions with k_3 from Gonzalez et al.,¹⁴ Meagher and Anderson,⁶ and Pham and Lin,¹⁵ respectively. Also calculations with the mechanism of Pham et al.¹³ are shown. The modeling was conducted assuming constant temperature and volume.

The observed differences are a consequence of the choices of both k_2 and k_3 . Pham et al. adopted k_2 from the study of Davidson et al.¹¹ However, as discussed above, their rate constant extrapolates poorly to lower temperature due to a too low activation energy. At 1083 K, the rate constant for R2 used by Pham et al. is thus almost three times faster than the values from Gonzalez et al. and Meagher and Anderson, which agree within 10%. To compensate for the enhanced NO formation rate from R2, a larger value of k_3 was required. Modeling with the present mechanism shows that the 1083 K experiment of Pham et al. is consistent with a very low value of k_3 .

Flow reactor experiments

Flow reactor results on N_2O decomposition and NO formation in N_2O /inert mixtures have been reported by several groups.⁶⁷⁻⁶⁹ These studies were all conducted at very dilute conditions and thus very sensitive to impurities. Figure 12 compares recent measurements by Liu et al.⁶⁸ with modeling predictions. They conducted experiments on decomposition of 400 ppm N_2O in Ar in a laminar flow alumina reactor over a wide range of temperature. The preferred mechanism with the rate constant of R3 from Gonzalez et al. overpredicts the NO formation. However, presence of just 5 ppm of H_2O lowers the predicted NO by up to a factor of four and brings the predictions with the low value of k_3 from Gonzalez et al. in agreement with experiment. Due to the uncertainty about the contamination, this type of experiment cannot be used to reliably determine the rate constant for R3.

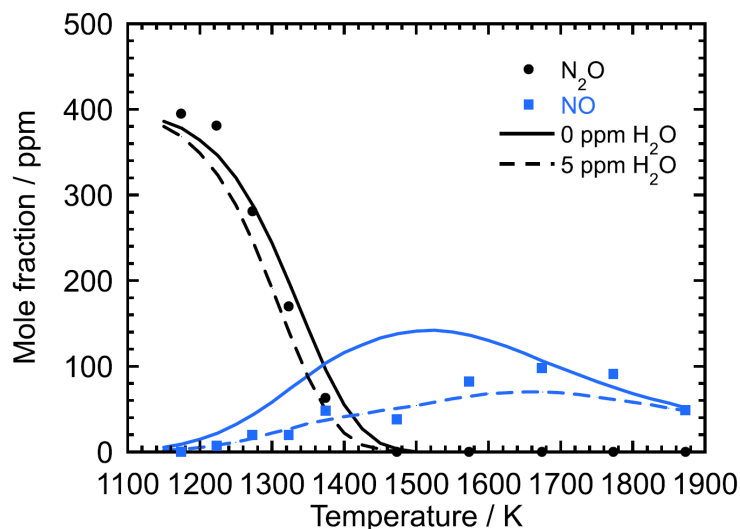


Figure 12: Comparison of the experimental data of Liu et al.⁶⁸ with modeling predictions for N_2O decomposition and NO formation in a N_2O /Ar mixture in a laminar flow reactor. Symbols denote experimental data, while lines denote modeling predictions. Inlet concentrations: $\text{N}_2\text{O} = 400$ ppm; balance Ar. The residence time is $450/T(\text{K})$ s. The pressure was not provided in the article, but it is assumed to be atmospheric.

Allen et al.⁷⁰ investigated decomposition of N_2O in a flow reactor as a function of residence time (location) at 1103-1173 K and 1.5-10.5 atm. Aware of the sensitivity to water vapor impurities, they added 600 ppm H_2O to the reactant mixture to ensure a known amount.

They monitored the N_2O consumption, along with formation of the products NO , O_2 , and NO_2 . Their results for NO and O_2 at 1103 K and 10.5 atm are compared with modeling predictions in Fig. 13.

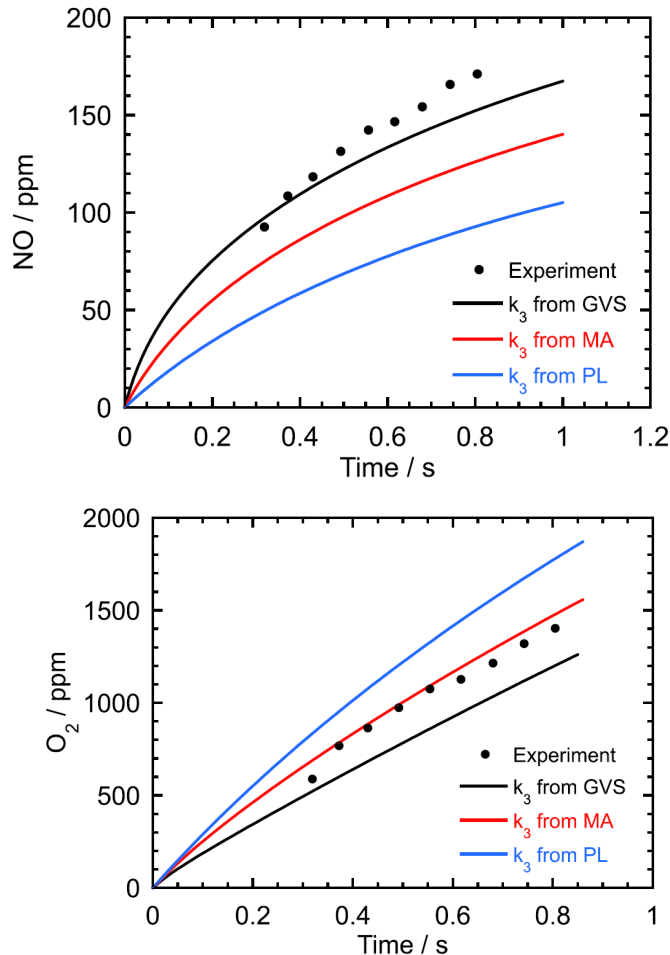


Figure 13: Comparison of the experimental data of Allen et al.⁷⁰ with modeling predictions for decomposition of N_2O in moist N_2 in a turbulent flow reactor at 1103 K and 10.5 atm. Symbols denote experimental data, while solid lines denote modeling predictions. Inlet concentrations: $\text{N}_2\text{O} = 1.0\%$, $\text{H}_2\text{O} = 557$ ppm; balance N_2 . Modeling predictions with k_3 from Gonzalez et al.¹⁴ (present model), Meagher and Anderson,⁶ and Pham and Lin,¹⁵ respectively.

A satisfactory prediction of the observed O_2 and NO profiles is obtained with the values of k_3 from Gonzalez et al. and Meagher and Anderson. The differences to experiment can largely be explained by uncertainties in secondary reactions (R1, R4). However, the discrepancy for both NO and O_2 is larger when adopting k_3 from Pham and Lin.

Implications for the $\text{N}_2\text{O} + \text{O}$ rate constant

Among the two product channels for $\text{N}_2\text{O} + \text{O}$,



the rate constant for R2 is well established. The evaluations of Baulch and coworkers,^{7,8} Hanson and Salimian,⁹ Tsang and Herron,¹⁰ and Meagher and Anderson,⁶ which were all based on measurements of both the forward and reverse reaction, agree closely, and they are consistent also with the theoretical values from Gonzalez et al.¹⁴ and Pham and Lin.¹⁵

The reported rate constants for $\text{N}_2\text{O} + \text{O} \rightleftharpoons \text{N}_2 + \text{O}_2$ (R3) are scattered and difficult to reconcile. They can roughly be divided into three groups according to activation energy:

- A low activation energy of 11-16 kcal mole⁻¹,^{6,7,11,13,15} consistent with reaction occurring on the singlet surface after intersystem crossing.¹⁵
- An activation energy roughly corresponding to that of R2, around 28 kcal mole⁻¹.^{4,8-10}
- A high activation energy of around 40 kcal mole⁻¹, roughly corresponding to the reported barrier on the triplet surface.^{14,15}

Based on the theoretical work by Gonzalez et al.¹⁴ and Pham and Lin,¹⁵ an activation energy for R2 of 28 kcal mole⁻¹, as proposed in the early evaluations,⁸⁻¹⁰ can be discarded. With a 40 kcal mole⁻¹ barrier, the direct reaction on the triplet surface is too slow for the $\text{N}_2 + \text{O}_2$ channel to have any practical significance. Thus the importance of R3 depends entirely on the alternative low barrier path involving intersystem crossing and reaction on the singlet surface. The issue is to what extent this path is active. To examine this, it is required to identify the experimental results that are at the same time reliable and sufficiently sensitive

to k_3 . The $\text{N}_2\text{O} + \text{O}$ reaction is comparatively slow and NO is easily affected by experimental artifacts that generally serve to suppress the NO yield and thereby result in an overestimation of k_3 .

Meagher and Anderson did a careful assessment of the available experimental results for $\text{N}_2\text{O} + \text{O}$. They discarded the early shock tube measurements due to impurity issues, as well as the $(d[\text{NO}]/dt)/(d[\text{N}_2\text{O}]/dt)$ data from batch reactors due to difficulties in obtaining accurate initial rates. While we agree with these reservations, contrary to Meagher and Anderson, we have confidence in the reported data for the final NO yield from the shock tube experiments of Zuev and Starikovskii⁵² and from the batch reactor work of Kaufman et al.¹⁶ and Lindars and Hinshelwood²⁵ (provided O-loss at the surface is accounted for). Unlike Meagher and Anderson, we choose to disregard the measurements of Fontijn et al.¹² Even though Fontijn et al. provided a careful analysis of the impact of impurities, the apparent conflict with the large majority of data examined in this work tends to indicate that there was an experimental problem.

Use of data for the final NO yield to derive rate constants for $\text{N}_2\text{O} + \text{O}$ (R2, R3) is complicated due to side reactions. In addition to the rates of thermal dissociation of N_2O (R1) and $\text{N}_2\text{O} + \text{O}$ (R2, R3), the NO yield is affected by removal of atomic oxygen by $\text{NO} + \text{O} (+\text{M}) \rightarrow \text{NO}_2 + \text{M}$ (R7) and $\text{NO}_2 + \text{O} \rightarrow \text{NO} + \text{O}_2$ (R8). Figure 14 shows the results of a sensitivity analysis with respect to NO for the conditions of a batch reactor experiment (Kaufman et al., 973 K, 50 torr; Fig. 9) and a shock tube experiment (Zuev and Starikovskii, 1800 K, 2.5 atm; Fig. 5). The calculations are conducted with the upper limit values for k_3 discussed below. With the preferred k_3 , the sensitivity coefficients for this reaction are essentially zero.

The reactions with the largest sensitivity coefficients are $\text{N}_2\text{O} + \text{O}$ (R2, R3) and $\text{NO} + \text{O} (+\text{M})$ (R7). Changes of the rate constants for $\text{N}_2\text{O} (+\text{M})$ (R1) and $\text{NO}_2 + \text{O}$ (R8) within their uncertainty limits (Table 1) have only a small impact on modeling predictions. For the batch reactor experiment with pure N_2O , the uncertainty in k_7 is increased since the collision

efficiency of N_2O in R7 has not been measured. Based on the NO measurements and their uncertainties, together with the uncertainty in the rate constants for the sensitive reactions (see Table 1), upper limits for k_3 for the two conditions were estimated. We find values of $3 \times 10^8 \text{ cm}^3 \text{ mol}^{-1} \text{ s}^{-1}$ (973 K) and $9 \times 10^9 \text{ cm}^3 \text{ mol}^{-1} \text{ s}^{-1}$ (1800 K), respectively; factors of 3-5 below the Meagher and Anderson recommendation and roughly an order of magnitude below the calculation of Pham and Lin.

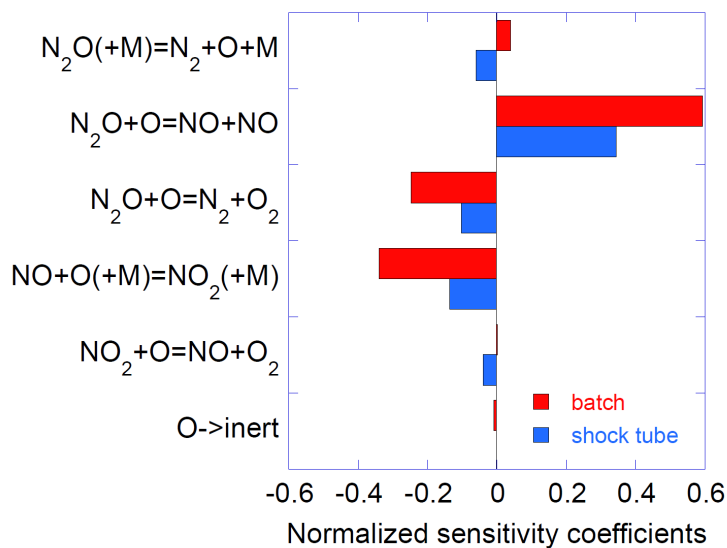


Figure 14: Sensitivity coefficients for NO for the conditions of Fig. 9 (batch reactor; 973 K, 50 torr) and Fig. 5 (shock tube; 1800 K, 2.5 atm). The analysis is conducted with the estimated upper limit values of k_3 .

Figure 15 shows the correlation between measured and predicted NO yields as a function of the chosen value of k_3 . The data cover batch reactor results at 973-1031 K and 0.013-0.66 atm from Kaufman et al.¹⁶ and Lindars and Hinshelwood²⁵ and shock tube data at 1800-2200 K and 2.5-11.5 atm from Zuev and Starikovskii.⁵² With the preferred mechanism, including the rate constant for R3 from Gonzalez et al., the agreement is excellent over the full range of pressure and temperature. With the pressure-dependent rate constant for $\text{NO} + \text{O} (+\text{M})$ (R7) being the major kinetic uncertainty, the observed agreement over a wide pressure range provides strong support for both k_3 and k_7 . Further support for k_3 is provided by measurements in the 1000-1100 K temperature range in batch reactors (Pham et al.¹³)

and shock tube work in the 1400-2200 K range (Davidson et al.¹¹ and Ross et al.³⁵)

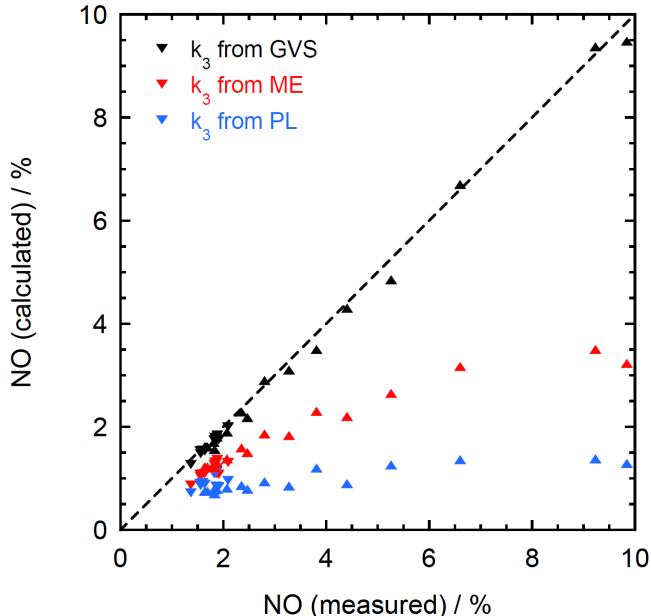


Figure 15: Correlation between predicted and measured final NO yield in thermal conversion of N_2O . The experimental data are drawn from the shock tube experiments of Zuev and Starikovskii⁵² (\blacktriangledown) and the batch reactor experiments of Lindars and Hinshelwood²⁵ and Kaufman et al.¹⁶ (\blacktriangle). The data cover pressures of 0.013-11.5 atm and temperatures of 973-2200 K. The symbols denote modeling predictions with k_3 from Gonzalez et al.,¹⁴ Meagher and Anderson,⁶ and Pham and Lin,¹⁵ respectively.

The present findings conflict with the theoretical work of Pham and Lin.¹⁵ However, there is some ambiguity in their treatment of the inter-system crossing in R3. At any crossing point, the singlet and triplet energies must be equal. We note that the geometry of MSX1, as reported by Pham and Lin from their CCSD/aug-cc-pVTZ calculations, does not satisfy this condition. At this geometry and level of theory the singlet wavefunction (the lowest energy singlet state is UHF with $\langle S^2 \rangle = 1.02$ rather than zero, whose high spin-contamination presumably arises from the $O(^1D)$ atom 2.0×10^{-10} m from N_2O) lies 15 kcal mol⁻¹ above the lowest triplet state ($\langle S^2 \rangle = 2.08$, close to ideal), while the RHF singlet is 36 kcal mol⁻¹ above the triplet. Application of CCSD(T)/aug-cc-pVTZ theory yields differences of 11 and 33 kcal mol⁻¹, respectively. These latter calculations indicate the triplet state to be 11 kcal mol⁻¹ above $O(^3P) + N_2O$, consistent with the past work, so

that the discrepancy likely centers on the singlet energy in the region of MSX1.

Another point of concern is that Pham and Lin calculate a probability of 100% for intersystem crossing. This value is much larger than proposed for some other reactions involving ISC, where the probability is 10% or less. For example, spin-forbidden R1 at the high-pressure limit has an experimental A factor $\sim 10^{11} \text{ s}^{-1}$, considerably smaller than is typical for spin-allowed dissociation reactions. We use the properties of the minimum-energy singlet-triplet crossing point for N_2O provided by Harvey and Aschi⁷¹ to evaluate $k_{1,\infty}$ by transition state theory, assuming an ISC probability of 1. An Arrhenius fit yields an A factor of 10^{15} s^{-1} . Comparison with experiment is therefore consistent with an average probability of ISC of around 0.01% for N_2O . For comparison, some spinforbidden reactions of sulfur atoms (that have greater spin-orbit coupling than oxygen) have estimated ISC probabilities of the order of 5%.⁷²

Concluding remarks

The rate constant for the reaction $\text{N}_2\text{O} + \text{O} \rightleftharpoons \text{N}_2 + \text{O}_2$ (R3) is difficult to quantify based on the available experimental and theoretical evidence. Reaction on the triplet surface is very slow due to a barrier of around 40 kcal mole⁻¹.^{14,15} It has been proposed that the reaction may proceed via inter-system crossing from the triplet to the singlet surface,¹⁵ involving a much lower activation energy.¹⁵ The present re-examination of available experimental results does not support a low barrier path for $\text{N}_2\text{O} + \text{O}$. A very good agreement between modeling predictions and most experimental results is obtained considering only reaction on the triplet surface. The present work indicates that the rate constant for R3 is considerably slower than values currently employed in modeling and that $\text{N}_2\text{O} + \text{O}$ will be of minor importance for removing N_2O under most practical conditions.

Supporting Information for Publication

Reaction mechanism and thermodynamic data for modeling.

Acknowledgements

The authors acknowledge support from the European Horizon 2020 program for the Engimonia project. PM was supported by the U.S. Department of Energy, Office of Basic Energy Sciences, Division of Chemical Sciences, Geosciences and Biosciences/Gas Phase Chemical Physics under Contract No. DESC0020952. Computational facilities were purchased, in part, with support from the National Science Foundation (Grant No. CHE-0741936).

References

- (1) Valera-Medina, A.; Xiao, H.; Owen-Jones, M.; David, W. I. F.; Bowen, P. J. Ammonia for power. *Prog. Energy Combust. Sci.* **2018**, *69*, 63–102.
- (2) Kobayashi, H.; Hayakawa, A.; Somarathne, K. K. A.; Okafor, E. C. Science and technology of ammonia combustion. *Proc. Combust. Inst.* **2019**, *37*, 109–133.
- (3) Valera-Medina, A. et al. A review on ammonia as a potential fuel: from synthesis to economics. *Energy Fuels* **2021**, *35*, 6964–7029.
- (4) Glarborg, P.; Miller, J. A.; Ruscic, B.; Klippenstein, S. J. Modeling nitrogen chemistry in combustion. *Prog. Energy Combust. Sci.* **2018**, *67*, 31–68.
- (5) Glarborg, P. The $\text{NH}_3/\text{NO}_2/\text{O}_2$ system: Constraining key steps in ammonia ignition and N_2O formation. *Combust. Flame* **2023**,
- (6) Meagher, N.; Anderson, W. Kinetics of the $\text{O}(^3\text{P}) + \text{N}_2\text{O}$ reaction. 2. Interpretation and recommended rate coefficients. *J. Phys. Chem. A* **2000**, *104*, 6013–6031.

- (7) Baulch, D.; Bowman, C.; Cobos, C.; Cox, R.; Just, T.; Kerr, J.; Pilling, M.; Stocker, D.; Troe, J.; Tsang, W.; Walker, R.; Warnatz, J. Evaluated kinetic data for combustion modeling: Supplement II. *J. Phys. Chem. Ref. Data* **2005**, *34*, 757–1397.
- (8) Baulch, D.; Drysdale, D.; Horne, D.; Lloyd, A. *Evaluated kinetic data for high temperature reactions. Vol 2, Homogeneous gas phase reactions of the H₂-N₂-O₂ system*; Butterworths, London, 1973.
- (9) Hanson, R.; Salimian, S. In *Combustion chemistry*; W.C. Gardiner, J., Ed.; Springer-Verlag, New York, 1984.
- (10) Tsang, W.; Herron, J. T. Chemical kinetic data base for propellant combustion I. Reactions involving NO, NO₂, HNO, HNO₂, HCN and N₂O. *J. Phys. Chem. Ref. Data* **1991**, *20*, 609–663.
- (11) Davidson, D. F.; DiRosa, M. D.; Chang, A. Y.; Hanson, R. K. Shock tube measurements of the major product channels of N₂O + O. *Shock Waves* **1992**, *2*, 813.
- (12) Fontijn, A.; Goumri, A.; Fernandez, A.; Anderson, W. R.; Meagher, N. E. Kinetics of the O(³P) + N₂O reaction. 1. Direct measurements at intermediate temperatures. *J. Phys. Chem. A* **2000**, *104*, 6003–6012.
- (13) Pham, T. V.; Tsay, T. J.; Lin, M. C. Thermal decomposition of N₂O near 900 K studied by FTIR spectrometry: Comparison of experimental and theoretical O (³P) formation kinetics. *Int. J. Chem. Kinet.* **2020**, *52*, 632–644.
- (14) González, M.; Valero, R.; Sayos, R. Ab initio ground potential energy surface (3A'') for the O (³P) + N₂O reaction and kinetics study. *J. Chem. Phys.* **2001**, *115*, 2540–2549.
- (15) Pham, T. V.; Lin, M. C. Investigation of Product Formation in the O(¹D, ³P) + N₂O Reactions: Comparison of Experimental and Theoretical Kinetics. *J. Phys. Chem. A* **2022**, *126*, 1103–1113.

- (16) Kaufman, F.; Gerri, N.; Bowman, R. Role of nitric oxide in the thermal decomposition of nitrous oxide. *J. Chem. Phys.* **1956**, *25*, 106–115.
- (17) Dindi, H.; Tsai, H.-M.; Branch, M. Combustion mechanism of carbon monoxide-nitrous oxide flames. *Combust. Flame* **1991**, *87*, 13–20.
- (18) Rohrig, M.; Petersen, E. L.; Davidson, D. F.; Hanson, R. K. The pressure dependence of the thermal decomposition of N₂O. *Int. J. Chem. Kinet.* **1996**, *28*, 599–608.
- (19) Marshall, P.; Ko, T.; Fontijn, A. High-temperature photochemistry kinetics studies of the reactions of hydrogen atom (12S) and deuterium atom (12S) with nitrous oxide. *J. Phys. Chem.* **1989**, *93*, 1922–1927.
- (20) Mebel, A. M.; Lin, M.-C.; Morokuma, K.; Melius, C. F. Theoretical study of reactions of N₂O with NO and OH radicals. *Int. J. Chem. Kinet.* **1996**, *28*, 693–703.
- (21) Bemand, P. P.; Clyne, M. A. A.; Watson, R. T. Atomic resonance fluorescence and mass spectrometry for measurements of the rate constants for elementary reactions: O³P + NO₂ → NO + O₂ and NO + O₃ → NO₂ + O₂. *J. Chem. Soc., Faraday Trans. 2: Molec. Chem. Phys.* **1974**, *70*, 564–576.
- (22) Javoy, S.; Mével, R.; Paillard, C. E. A study of N₂O decomposition rate constant at high temperature: Application to the reduction of nitrous oxide by hydrogen. *Int. J. Chem. Kinet.* **2009**, *41*, 357–375.
- (23) Mulvihill, C. R.; Alturaifi, S. A.; Petersen, E. L. A shock-tube study of the N₂O + M ⇌ N₂ + O + M (M = Ar) rate constant using N₂O laser absorption near 4.6 μm. *Combust. Flame* **2021**, *224*, 6–13.
- (24) Johnston, H. S. Interpretation of the data on the thermal decomposition of nitrous oxide. *J. Chem. Phys.* **1951**, *19*, 663–667.

- (25) Lindars, F. J.; Hinshelwood, C. N. The thermal decomposition of nitrous oxide I. Secondary catalytic and surface effects. *Proc. Royal Soc. London. Series A. Math. Phys. Sci.* **1955**, *231*, 162–178.
- (26) Koshi, M.; Asaba, T. Shock-tube study of thermal decomposition of nitric oxide between 2700 and 3500 K. *Int. J. Chem. Kinet.* **1979**, *11*, 305–315.
- (27) Thielen, K.; Roth, P. Resonance absorption measurements of N and O atoms in high temperature NO dissociation and formation kinetics. *Symp. (Int.) Combust.* **1985**, *20*, 685–693.
- (28) McCullough, R. W.; Kruger, C. H.; Hanson, R. K. A flow tube reactor study of thermal decomposition rates of nitric oxide. *Combust. Sci. Technol.* **1977**, *15*, 213–223.
- (29) Wise, H.; Frech, M. F. Kinetics of decomposition of nitric oxide at elevated temperatures. II. The effect of reaction products and the mechanism of decomposition. *J. Chem. Phys.* **1952**, *20*, 1724–1727.
- (30) Kaufman, F.; Kelso, J. R. Thermal decomposition of nitric oxide. *J. Chem. Phys.* **1955**, *23*, 1702–1707.
- (31) Monat, J. P.; Hanson, R. K.; Kruger, C. H. Kinetics of nitrous oxide decomposition. *Combust. Sci. Technol.* **1977**, *16*, 21–28.
- (32) Dean, A. M.; Steiner, D. C. A shock tube study of the recombination of carbon monoxide and oxygen atoms. *J. Chem. Phys.* **1977**, *66*, 598–604.
- (33) Zaslonko, I. S.; Mozhukhin, E. V.; Mukoseev, Y. K.; Smirnov, V. N. Nonequilibrium reaction between N₂O and CO in shock waves. *Combust. Explos. Shock Waves* **1978**, *14*, 218–224.
- (34) Zaslonko, I.; Losev, A. S.; Mozhukhin, E. V.; Mukoseev, Y. K. Thermal decomposition of N₂O in Ar, He, N₂, or CO atmospheres. *Kinet. Catal.* **1980**, *21*, 236–240.

- (35) Ross, S. K.; Sutherland, J. W.; Kuo, S.-C.; Klemm, R. B. Rate constants for the thermal dissociation of N₂O and the O(³P) + N₂O reaction. *J. Phys. Chem. A* **1997**, *101*, 1104–1116.
- (36) Bedjanian, Y.; Kalyan, C. Rate constants of the reactions of O (³P) atoms with Br₂ and NO₂ over the temperature range 220–950 K. *Int. J. Chem. Kinet.* **2019**, *51*, 476–483.
- (37) Li, Y.; Javoy, S.; Mevel, R.; Xu, X. A chemically consistent rate constant for the reaction of nitrogen dioxide with the oxygen atom. *Phys. Chem. Chem. Phys.* **2021**, *23*, 585–596.
- (38) Fenimore, C. P.; Jones, G. W. Rate of the reaction, O + N₂O → 2NO. *Symp. (Int.) Combust.* **1961**, *8*, 127–133.
- (39) Bradley, J. N.; Kistiakowsky, G. B. Shock wave studies by mass spectrometry. I. Thermal decomposition of nitrous oxide. *J. Chem. Phys.* **1961**, *35*, 256–263.
- (40) Jost, W.; Michel, K. W.; Troe, J.; Wagner, H. G. Untersuchung des thermischen Zerfalls von N₂O in Stoßwellen. *Zeit. Naturforsch. A* **1964**, *19*, 59–64.
- (41) Fishburne, E. S.; Edse, R. Shock-tube study of nitrous oxide decomposition. *J. Chem. Phys.* **1964**, *41*, 1297–1304.
- (42) Olschewski, H. A.; Troe, J.; Wagner, H. G. Niederdruckbereich und Hochdruckbereich des unimolekularen N₂O-Zerfalls. *Ber. Bunsenges. Phys. Chem.* **1966**, *70*, 450–459.
- (43) Gutman, D.; Belford, R. L.; Hay, A. J.; Pancirov, R. Shock Wave Studies with a Quadrupole Mass Filter. II. The Thermal Decomposition of Nitrous Oxide. *J. Phys. Chem.* **1966**, *70*, 1793–1800.
- (44) Borisov, A. A. Thermal decomposition of N₂O at high temperatures. *Kinet. Katal.* **1968**, *9*, 482.

- (45) Barton, S. C.; Dove, J. E. Mass spectrometric studies of chemical reactions in shock waves: the thermal decomposition of nitrous oxide. *Can. J. Chem.* **1969**, *47*, 521–538.
- (46) Lipkea, W. H.; Milks, D.; Matula, R. A. Nitrous oxide decomposition and its reaction with atomic oxygen. *Combust. Sci. Technol.* **1973**, *6*, 257–267.
- (47) Dove, J. E.; Nip, W. S.; Teitelbaum, H. The vibrational relaxation and pyrolysis of shock heated nitrous oxide. *Symp. (Int.) Combust.* **1975**, *15*, 903–916.
- (48) Baber, S. C.; Dean, A. M. N₂O dissociation behind reflected shock waves. *Int. J. Chem. Kinet.* **1975**, *7*, 381–398.
- (49) Dean, A. M. Shock tube studies of the N₂O/Ar and N₂O/H₂/Ar systems. *Int. J. Chem. Kinet.* **1976**, *8*, 459–474.
- (50) Fujii, N.; Sagawai, S.; Sato, T.; Nosaka, Y.; Miyama, H. Study of the thermal dissociation of nitrous oxide and carbon dioxide using oxygen (³P) atomic resonance absorption spectroscopy. *J. Phys. Chem.* **1989**, *93*, 5474–5478.
- (51) Michael, J. V.; Lim, K. P. Rate constants for the N₂O reaction system: Thermal decomposition of N₂O; N + NO → N₂ + O; and implications for O + N₂ → NO + N. *J. Chem. Phys.* **1992**, *97*, 3228–3234.
- (52) Zuev, A. P.; Starikovskii, A. Y. Reactions involving nitrogen oxides at high temperature. Reactions of N₂O with atomic oxygen. *Sov. J. Chem. Phys.* **1992**, *10*, 255–272.
- (53) Lin, M.-C.; Bauer, S. H. Bimolecular Reaction of N₂O with CO and the Recombination of O and CO as Studied in a Single-Pulse Shock Tube. *J. Chem. Phys.* **1969**, *50*, 3377–3391.
- (54) Milks, D.; Matula, R. A. A single-pulse shock-tube study of the reaction between nitrous oxide and carbon monoxide. *Symp. (Int.) Combust.* **1973**, *14*, 83–97.

- (55) Fujii, N.; Kakuda, T.; Sugiyama, T.; Miyama, H. Direct determination of the rate constant for the reaction $\text{CO} + \text{N}_2\text{O} \rightarrow \text{CO}_2 + \text{N}_2$. *Chem. Phys. Lett.* **1985**, *122*, 489–492.
- (56) Fujii, N.; Kakuda, T.; Takeishi, N.; Miyama, H. Kinetics of the high temperature reaction of carbon monoxide with nitrous oxide. *J. Phys. Chem.* **1987**, *91*, 2144–2148.
- (57) Starikovskii, A. Y. Kinetics and mechanism of reaction in N_2O – CO system at high temperatures. *Khim. Fiz.* **1994**, *13*, 94–120.
- (58) Loirat, H.; Caralp, F.; Destriau, M.; Lesclaux, R. Oxidation of carbon monoxide by nitrous oxide between 1076 and 1228 K: determination of the rate constant of the exchange reaction. *J. Phys. Chem.* **1987**, *91*, 6538–6542.
- (59) Wang, Y.; Fu, G.; Zhang, Y.; Xu, X.; Wan, H. O-atom transfer reaction from N_2O to CO : A theoretical investigation. *Chem. Phys. Lett.* **2009**, *475*, 202–207.
- (60) Bacskay, G. B.; Mackie, J. C. Oxidation of CO by SO_2 : A theoretical study. *J. Phys. Chem. A* **2005**, *109*, 2019–2025.
- (61) Musgrave, F. F.; Hinshelwood, C. N. The thermal decomposition of nitrous oxide, and its catalysis by nitric oxide. *Proc. Royal Soc. London. Ser. A* **1932**, *135*, 23–39.
- (62) Lindars, F. J.; Hinshelwood, C. N. The thermal decomposition of nitrous oxide II. Influence of added gases and a theory of the kinetic mechanism. *Proc. Royal Soc. London. Series A. Math. Phys. Sci.* **1955**, *231*, 178–197.
- (63) Lewis, R. M.; Hinshelwood, C. N. The thermal decomposition of nitrous oxide. *Proc. Royal Soc. London. Series A.* **1938**, *168*, 441–454.
- (64) Loirat, H.; Caralp, F.; Forst, W.; Schoenenberger, C. Thermal unimolecular decomposition of nitrous oxide at low pressures. *J. Phys. Chem.* **1985**, *89*, 4586–4591.

- (65) Johnsson, J. E. Formation and reduction of nitrogen oxides in fluidized-bed combustion. *Fuel* **1994**, *73*, 1398–1415.
- (66) Glarborg, P.; Hashemi, H.; Cheskis, S.; Jasper, A. W. On the rate constant for $\text{NH}_2 + \text{HO}_2$ and third-body collision efficiencies for $\text{NH}_2 + \text{H} (+ \text{M})$ and $\text{NH}_2 + \text{NH}_2 (+ \text{M})$. *J. Phys. Chem. A* **2021**, *125*, 1505–1516.
- (67) Hulgaard, T.; Dam-Johansen, K. Homogeneous nitrous oxide formation and destruction under combustion conditions. *AIChE J.* **1993**, *39*, 1342–1354.
- (68) Liu, S.; Fan, W.; Guo, H.; Wu, X.; Chen, J.; Liu, Z.; Wang, X. Relationship between the N_2O decomposition and NO formation in $\text{H}_2\text{O}/\text{CO}_2/\text{NH}_3/\text{NO}$ atmosphere under the conditions of simulated air-staged combustion in the temperature interval of 900–1600 °C. *Energy* **2020**, *211*, 118647.
- (69) Lee, S. J.; Yun, J. G.; Lee, H. M.; Kim, J. Y.; Yun, J. H.; Hong, J. G. Dependence of $\text{N}_2\text{O}/\text{NO}$ Decomposition and Formation on Temperature and Residence Time in Thermal Reactor. *Energies* **2021**, *14*, 1153.
- (70) Allen, M. T.; Yetter, R. A.; Dryer, F. L. The decomposition of nitrous oxide at $1.5 \leq P \leq 10.5$ atm and $1103 \leq T \leq 1173$ K. *Int. J. Chem. Kinet.* **1995**, *27*, 883–909.
- (71) Harvey, J. N.; Aschi, M. Spin-forbidden dehydrogenation of methoxy cation: a statistical view. *Phys. Chem. Chem. Phys.* **1999**, *1*, 5555–5563.
- (72) Ayling, S.; Gao, Y.; Marshall, P. Kinetic studies of the reaction of atomic sulfur with acetylene. *Proc. Combust. Inst.* **2015**, *35*, 215–222.

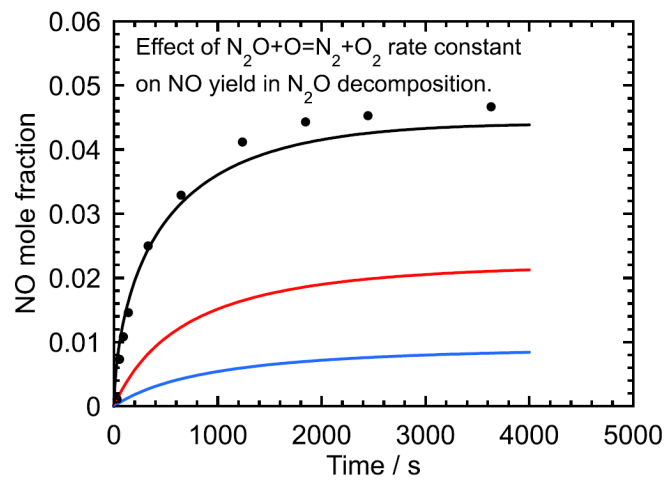


Figure 16: TOC graphic